sustainability

MDPI

Article

Solution Combustion Synthesis of Transparent Conducting Thin Films for Sustainable Photovoltaic Applications

Sana Ullah [1,2,*], Rita Branquinho [1], Tiago Mateus [3], Rodrigo Martins [3], Elvira Fortunato [1], Tahir Rasheed [4,*] and Farooq Sher [5,*]

1 CENIMAT/I3N, Departamento de Ciência dos Materiais (The Materials Science Department), Faculdade de Ciências e Tecnologia (Faculty of Science and Technology, FCT), Universidade Nova de Lisboa (Universidade Nova de Lisboa, UNL), 2829-516 Caparica, Portugal; ritasba@fct.unl.pt (R.B.); emf@fct.unl.pt (E.F.)

2 Deparment of Physics, Khwaja Fareed Universiy of Engineering and Information Technology (KFUEIT), Rahim Yar Khan, 64200 Punjab, Pakistan

3 CEMOP, Departamento de Ciência dos Materiais (The Materials Science Department), Faculdade de Ciências e Tecnologia (Faculty of Science and Technology, FCT), Universidade Nova de Lisboa (Universidade Nova de Lisboa, UNL), 2829-516 Caparica, Portugal; tp.mateus@gmail.com (T.M.); rm@uninova.pt (R.M.)

4 School of Chemistry and Chemical Engineering, Shanghai Jiao Tong University, Shanghai 200240, China

5 Faculty of Engineering, Environmental and Computing, School of Mechanical, Aerospace and Automotive Engineering, Coventry University, Coventry CV1 5FB, UK

* Correspondence: Sana.Ullah@kfueit.edu.pk (S.U.); masil@sjtu.edu.cn (T.R); Farooq.Sher@coventry.ac.uk (F.S.)

Received: 8 November 2020; Accepted: 7 December 2020; Published: 13 December 2020

Abstract: Sunlight is arguably the most promising continuous and cheap alternative sustainable energy source available at almost all living places of the human world. Photovoltaics (PV) is a process of direct conversion of sunlight into electricity and has become a technology of choice for sustainable production of cleaner and safer energy. The solar cell is the main component of any PV technology and transparent conducting oxides (TCO) comprising wide band gap semiconductors are an essential component of every PV technology. In this research, transparent conducting thin films were prepared by solution combustion synthesis of metal oxide nitrates wherein the use of indium is substituted or reduced. Individual 0.5 M indium, gallium and zinc oxide source solutions were mixed in ratios of 1:9 and 9:1 to obtain precursor solutions. Indium-rich IZO (A1), zinc-rich IZO (B1), gallium-rich GZO (C1) and zinc-rich GZO (D1) thin films were prepared through spin coating deposition. In the case of A1 and B1 thin films, electrical resistivity obtained was 3.4×10^{-3} Ω-cm and 7.9×10^{-3} Ω-cm, respectively. While C1 films remained insulating, D1 films showed an electrical resistivity of 1.3×10^{-2} Ω-cm. The optical transmittance remained more than 80% in visible for all films. Films with necessary transparent conducting properties were applied in an all solution-processed solar cell device and then characterized. The efficiency of 1.66%, 2.17%, and 0.77% was obtained for A1, B1, and D1 TCOs, respectively, while 6.88% was obtained using commercial fluorine doped SnO_2: (FTO) TCO. The results are encouraging for the preparation of indium-free TCOs towards solution-processed thin-film photovoltaic devices. It is also observed that better filtration of precursor solutions and improving surface roughness would further reduce sheet resistance and improve solar cell efficiency.

Keywords: sustainability; solution combustion synthesis; renewables; rapid thermal annealing and photovoltaics

1. Introduction

The human world foresees acute energy shortage. Depleting fossil fuel reservoirs coupled with their adverse climatic effects compel us to seek alternative and sustainable energy sources. Among possible alternatives, solar energy is arguably the most promising and sustainable being a continuous and cheap source available at almost all living places of the world. Photovoltaics (PV) is a process of direct conversion of sunlight into electricity. Since its discovery by Edmond Becquerel in 1839, PV has become a method of choice for the production of cleaner and safer energy and holds promise to sustain future energy demands. Sun provides almost 5×10^{24} J of energy each year that is 10,000 times more than the present energy consumption of the world [1]. Solar photovoltaics has already achieved an installed capacity of approximately 400 GW at the end of 2017 [2] and is expected to rise to TW levels this decade [3]. PV system comprises many components like mechanical and electrical auxiliary connections. A solar cell, the main component of the PV system, plays the central and pivotal role. Transparent conducting oxides (TCO) comprising wide band gap semiconductors combining unique characteristics of conductivity and transparency are an essential component of almost every photovoltaic technology. These are applied as front contact layers to allow sunlight to reach absorber material for the production of charge careers and generation of electricity. TCOs, needed to have lower electrical resistivity combined with greater optical transparency in the visible, are the basic component of thin-film based photovoltaic (PV) technologies [4–6]. These are particularly required for continually increasing market demand for liquid crystal displays (LCD), smart windows, touch screens, and flat panel displays [7].

In simplistic of these devices, TCO acts as a contact electrode for transmission across a visible spectrum of light. Indium tin oxide (ITO) is the industry standard even though its characteristics remain stagnant over the period of time [8]. ITO has been in widespread use and as per the most recent report [9], indium tin oxide held more than 93% of the market share. ITO thin films with required characteristics are usually obtained through vacuum intensive deposition methods. In these ITO thin films, indium is more than 90% in composition [10] and is an increasingly expensive and scarce element [11]. Alternative TCO materials with substituted or reduced use of indium having desired opto-electrical characteristics are being developed through vacuum-intensive physical vapor deposition methods like magnetron sputtering [12], radio frequency [13], and direct current [14,15] sputtering along with atomic layer deposition [16], aerosol assisted [17], atmospheric pressure [18], and chemical vapor deposition methods. These electrodes are also obtained through solution processes like spin-coating [19,20], dip-coating [21], and spray pyrolysis [22–24]. With ever-increasing market for transparent electrodes, search for alternative materials to sustain demands is on a continuous rise. TCOs obtained with substituted or reduced use of indium using vacuum-free deposition methods are need of the hour. Fluorine-doped tin oxide (FTO, SnO2: F) is another alternative in use, however, higher surface roughness [25] and brittle [5] properties reduce its usefulness. Furthermore, impurity-doped zinc oxide (ZnO) thin films, mainly aluminium and gallium doped ZnO (AZO and GZO), are the most sought after alternatives and have achieved a status of best alternative transparent conductive oxide materials to replace indium tin oxide (ITO) [8,26].

Here, this study presents a successful effort to synthesize alternative TCOs to reduce or substitute the use of indium in preparation of transparent conducting thin films for alternative and sustainable energy production. Present research directly addresses Goal 7, which ensures access to affordable, reliable, sustainable, and modern energy for all, of Resolution A/RES/70/1 Transforming our world: The 2030 Agenda for Sustainable Development adopted in the seventieth session of United Nations General Assembly on 25 September 2015.

2. Materials and Methods

In this work, indium and gallium zinc oxide thin films (IZO and GZO) were synthesized. Oxide source solutions in 0.5 M were prepared and then mixed in varying ratios to obtain precursor solutions for indium-rich IZO (A1), zinc-rich IZO (B1), gallium-rich GZO (C1), and zinc-rich GZO

(D1) thin films. Solution combustion synthesis (SCS), a variant of solution synthesis with its exothermic character, offers the advantage of conversion of ingredients into oxides at low pre-deposition temperatures. A source material used as fuel generates local heats for the conversion of precursors into oxides. The process has recently been exploited for low-temperature preparation of transparent and conducting IZO films [27]. Post-deposition rapid thermal annealing (RTA) has been demonstrated for its effectiveness in imparting desired opto-electrical characteristics to films in a relatively short time of application [28].

Herein, both of these have been exploited to prepare transparent conducting thin films with successful effort to substitute or reduce the use of indium. These TCO thin films have then been applied in a-Si thin-film PV device wherein many of the constituent layers were deposited at room temperature. Higher optical transparency is achieved at very low thicknesses of 200 nm of the prepared thin films as compared to typical TC thin film thickness of 150–350 nm [10]. Higher comparative efficiency, Jsc, Voc with lower Rsh has been demonstrated for B1 TCO based device. Encouraging is the fact that margin available to increase thickness keeping required optical transmission would allow reducing sheet resistance of TCO films. This could help to reduce the resistance of the cell and further improve efficiency.

2.1. Precursor Solution Preparation

In a variety of works, the respective concentration or amount of indium is more than 80% in the total concentration of the precursor. In preparation of indium zinc oxide thin films by radio frequency magnetron sputtering, the ratio of In: Zn was kept at 90:10 wt.% [29]. In an attempt to prepare boron-doped indium-boron-zinc-oxide (IBZO) thin films by spin-coating deposition, indium concentration was kept at 70% [30]. In another work [31], thin films were spin-coated from IZO solution of molar ratio 7:3. Tungsten doped IZO (WIZO) thin films were prepared from WO_3 and IZO (at 1:1%) sputtering targets using a radio frequency sputtering system [32]. In the work of [33], the nominal volume ratio of the In/Zn was arranged at 10%. The objective of this study was to reduce or avoid the use of scarce indium material. Therefore, the stoichiometric ratio of ingredients selected in the preparation of indium alternative TCOs keeping in view the sustainability aspect vis-à-vis reducing or avoiding the use of scare "indium" element.

Individual indium oxide, gallium oxide, and zinc oxide source solutions in concentrations of 0.5 M were prepared through combustion chemistry. These individual source solutions were mixed in 1:9 and 9:1 proportions to obtain thin-film precursor solutions. Either indium nitrate hydrate (In $(NO_3)_3{\cdot}xH_2O$, Sigma, 99.9 %), zinc nitrate hydrate (Zn $(NO_3)_2{\cdot}xH_2O$, Sigma, 98 %), or gallium nitrate hydrate ($(GaNO_3)_3.xH_2O$, Sigma 99.9 %) and urea (CO $(NH_2)_2$, Sigma, 98%) were mixed in 1:2.5 or 1:1.6 or 1:2.5 molar proportions, respectively in 2-methoxyethanole (2-ME, $C_3H_8O_2$, Fluka, 99%) to obtain 0.5 M solutions. These individual solutions were stirred on a magnetic stirrer for 2 hours at 60 °C and kept for 2 days at room temperature to age. These individual oxide source solutions were then mixed in proportions of 9:1 and 1:9 to yield indium-rich IZO (A1) and zinc-rich IZO (B1) thin-film precursor solutions, respectively. Details of precursor solutions and oxide source solutions mixing ratios are given in Table 1.

Table 1. Oxide source mixing ratios for precursor solutions.

Sample ID	Oxide Source Mixing Ratios
In-rich IZO (A1)	In:Zn = 9:1
Zn-rich IZO (B1)	In:Zn = 1:9
Ga-rich GZO (C1)	Ga:Zn = 9:1
Zn-rich GZO (D1)	Ga:Zn = 1:9

Similarly, individual oxide source solutions were mixed in the same composition proportions to yield precursor solutions for gallium-rich GZO (C1) and zinc-rich GZO (D1) thin films. All precursor solutions were homogenized by stirring at 60 °C for 10 min on a magnetic stirrer and allowed to cool down to room temperature for deposition of thin films through spin coating. All these solutions were used without any filtration or purification.

2.2. Thin Film Deposition

Thin films were prepared by spin-coating deposition on corning glass substrates from precursor solutions prepared as described in Section 2.1. However, before spin-coating deposition, Corning glass 7059 substrates cut into 3 × 3 cm dimensions were cleaned in an ultrasonic bath at 60 °C in acetone for 15 min, followed by cleaning in 2-isopropanol for 15 min and followed by drying by N_2. All substrates were placed in a PSD-UV Novascan system for 30 min to perform surface activation by UV/Ozone treatment. Thin films were deposited by sequentially spin-coating 10 layers from each precursor solution at 3000 rpm for 30 seconds (Laurell Technologies). Each layer deposition followed a consolidation treatment at 400 °C for 10 min on hot-plate at ambient and obtained thin film stacks were annealed in vacuum/O_2/N_2-5%H_2 at 600 °C for 10 min in an RTA system.

2.3. Thin Film Characterization

Thin films were prepared mainly for their use as TCO in thin-film based photovoltaic devices. All these films were, therefore, first characterized for electrical resistivity and then for optical transparency, two main requirements of a TCO. Gallium-rich GZO films showed higher electrical resistivity as measured by four-point probe resistivity measurement, these were not further characterized. TCO thin films from compositions of indium-rich IZO, zinc-rich IZO and zinc-rich GZO were applied in a solar cell device and characterized for photovoltaic properties. X-ray diffraction analysis was used to determine the structure of thin films using Panalytical X'Pert PRO diffractometer in Bragg–Brentano (θ/2θ coupled) geometry with Cu Kα line radiation (λ = 1.540598 Å). Optical characterization of thin films was performed by measuring total optical transmission using a Perkin Lambda 950 UV/VIS/NIR Spectrometer. Electrical characterizations were first carried out by Jandel Instruments Four Probe instrument and then by Hall Effect (HE) measurements in Van der Pauw geometry at room temperature using BioRad HL5500 HE system with a constant magnetic field of 0.5 T to determine electrical resistivity (ρ), Hall mobility (μ), and carrier concentration (n). Surface morphology was observed by scanning electron microscopy (SEM-FIB, Zeiss Auriga Crossbeam microscope).

2.4. Solar Cell Device: Structure and Characterization

Thin films of A1, B1 and D1 composition were eventually used as (Sana) TCO in a typical silicon photovoltaic (PV) device. Amorphous Si-based PV device was prepared comprising of Al/AZO/p-p-i-n-n/AZO/TCO (Sana) (A1, B1, D1) layers. For comparison, FTO was used as TCO in a similar device. Al electrode along with AZO layer was deposited at room temperature while p and n amorphous Si layers were deposited at 170 °C. J—V (short circuit current density Jsc and open-circuit voltage Voc) photoelectric conversion measurements of solar cell were done by current density (mA-cm^{-2}) vs. voltage (V) measurement using SPI-SUN Simulator 240 A equipped with Xenon lamp filtered to AM1.5 Global Spectrum (ASTM E-297). Solar cell structure characterized for photovoltaic properties with FTO and Sana TCO is reproduced in Figure 1.

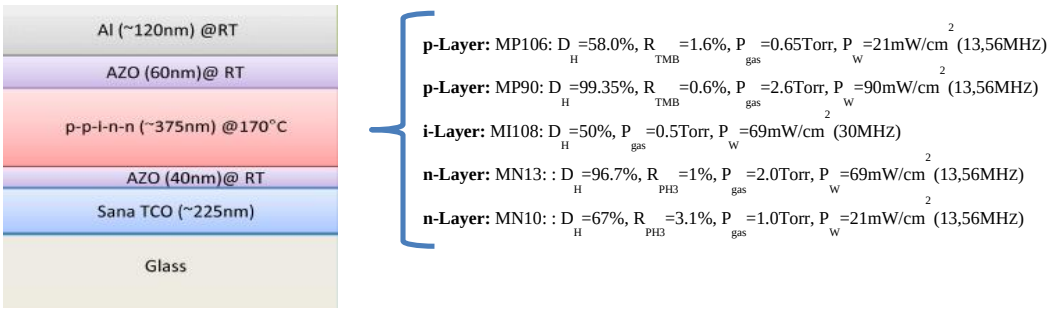

Figure 1. Depiction of solar cell structure with transparent conducting oxides (TCO) prepared in this work along with other layers characterized for photovoltaics (PV) properties.

Solution synthesis facilitates the preparation of a variety of precursors for vacuum-free deposition of thin films. Solution combustion synthesis (SCS) is a process of exothermic chemical reaction wherein oxidizing source is mixed in a reducing agent to generate local energy to convert precursors into oxides at lower process temperature [34]. Metal oxides are obtained by the chemical reaction between sources of metal oxide ions. Metal oxide source decomposition reaction and fuel oxidation reaction make the complete SCS reaction [35]. The decomposition reactions for zinc oxide, indium oxide, and gallium oxide along with decomposition of fuel (urea) are given in Equations (1) to (4).

$$Zn(NO_3)_2.-xH_2O \rightarrow ZnO + xH_2O + N_2 + (\frac{5}{2})O_2 \quad (1)$$

$$2In(NO_3)_3.-xH_2O \rightarrow In_2O_3 + xH_2O + 3N_2 + (\frac{15}{2})O_2 \quad (2)$$

$$Ga(NO_3)_2.-xH_2O \rightarrow GaO + xH_2O + N_2 + (\frac{5}{2})O_2 \quad (3)$$

$$CO(NH_2)_2 + (\frac{3}{2})O_2 \rightarrow 2H_2O + CO_2 + N_2 \quad (4)$$

The combined In_2O_3, ZnO, GaO and urea oxidation reduction reactions are presented in Equations (5) to (7).

$$3Zn(NO_3)_2.-xH_2O + 5CO(NH_2)_2 \rightarrow 3ZnO + xH_2O + 5CO_2 + 8N_2 \quad (5)$$

$$2In(NO_3)_3.-xH_2O + 5CO(NH_2)_2 \rightarrow In_2O_3 + xH_2O + 5CO_2 + 8N_2 \quad (6)$$

$$Ga(NO_3)_2.-xH_2O + 5CO(NH_2)_2 \rightarrow GaO + xH_2O + 6N_2 + (\frac{15}{2})O_2 \quad (7)$$

These reference equations helped to determine stoichiometric conditions for the redox reactions involved in the preparation of precursor solutions for deposition of IZO and GZO thin films. However, secondary reactions that are not accounted for herein can occur [26]. Selected reagents, oxidizer-fuel ratio (Φ) and chemistry of the redox reaction control thermodynamics for the formation of required oxides. Reducing/oxidizing valences (RV/OV) of reagents and their molar ratio (n) determine redox stoichiometry of the reaction as presented in Equation (8) [35,36].

$$\Phi = \frac{RV}{OV}n \quad (8)$$

The optimal molar stoichiometry (n = number of moles of fuel per mole of oxidizer) is obtained for $\Phi = 1$, which occurs when no molecular oxygen is required for the redox reaction. The reducing/oxidizing valences (RV/OV) are derived from propellant chemistry and determined by Jain et al. method [28]. In this method, elements are considered as either reducing or oxidizing. Reducing elements include carbon with RV = +4, hydrogen with RV = +1 and metal ions Mx+ with RV

= +x. Oxidizers include oxygen with OV= −2 and nitrogen with OV=0 [37,38]. The area has a reducing valence of RV = +6 and oxidizing valences of indium nitrate, zinc nitrate, and gallium nitrate are −15, −10, and −15, respectively. To assure redox stoichiometry, 1.6 moles of urea are required per mole of zinc nitrate, while 2.5 moles of urea are required per mole of indium nitrate and gallium nitrate, respectively. The urea to metal nitrate molar ratios were maintained constant while investigating the influence of In to Zn and Ga to Zn ratios and metal ion concentration of precursor solutions on the properties of IZO and GZO thin films.

Indium oxide, zinc oxide, and gallium oxide source solutions were prepared separately in 0.5 M concentration. These oxide source solutions were mixed in In: Zn and Ga: Zn ratios of 1:9 and 9:1 to yield IZO and GZO precursor solutions, respectively. IZO and GZO thin films were deposited by spin-coating and the number of layers were the same for all samples as such thickness of films remained similar (200 nm). All samples were provided similar pre- and post-deposition annealing treatments, as described in Section 2.2. Post-deposition rapid thermal annealing was provided in a vacuum, oxidizing (O_2), and N_2-5%H_2 environments. Thin films with better electrical conductivity obtained in the case of RTA in vacuum were applied in solar cell device and characterized.

3. Results and Discussion

3.1. XRD Structural Analysis

Crystal structure of film stacks was determined by X-ray diffraction analysis in 2θ range of 20°–80°. Figure 2 shows diffraction peaks obtained in the case of A1, B1, and D1 thin films. It is confirmed that all these films were of polycrystalline structure. Spin coating deposition parameters, pre- and post-deposition annealing temperatures, environment, and time were the same. Therefore, the only difference in precursor compositions affected the crystalline structure of thin films. Indium oxide normally develops in characteristic cubic bixbyite structure with preferential growth orientation peak of (222) along with minor orientation peaks according to JCPDS no. 06-041. Zinc oxide, on the other hand, stabilizes in characteristic hexagonal wurtzite structure with preferential growth orientation peak of (002) along with minor peaks, according to JCPDS no. 36-1415.

Moreover, it has been observed that GZO XRD characteristics are similar to that of ZnO and it crystallizes in (002) preferred orientation [39] even under different annealing temperatures and compositions [40,41]. The preferred peak (002), however, decreases in intensity with increasing gallium content along with some deviation in orientation angle as per competing ionic radii of constituents [42]. In the case of A1 thin films deposited from In: Zn 9:1 oxide source solutions' mixing ratio, characteristic In_2O_3 cubic bixbyite structure with preferred (222) orientation resulted in addition to minor peaks of (400) and (440) appearing at particular angles. This confirms the homogeneous mixing of zinc oxide source solution into the indium oxide source solution to render the preferred single phase of In_2O_3. No secondary phase of zinc-based compounds appeared. In the case of B1 thin films deposited from In: Zn 1:9 oxide source solutions mixing ratio, characteristic ZnO hexagonal wurtzite structure with preferred (002) orientation resulted in addition to minor characteristic orientation peaks of (100) and (101) appear at particular angles. Here, no secondary phase resulted for In_2O_3.

The respective XRD measurements confirmed appearing of individual phases for In_2O_3 and ZnO in thin films from In: Zn 1:9 and 9:1 precursor solutions, respectively. In the case of samples A1, characteristic In_2O_3 peak of (222) appeared prominent but for ZnO, the characteristic and minor peaks remained diminished. That could be because of the difference in ionic radii of In^{3+} (0.094 nm) and Zn^{2+} (0.074 nm) and precursor composition [43]. In the case of D1 thin films deposited from Ga: Zn 1:9 oxide source solutions' mixing ratio, characteristic ZnO major and minor peaks appeared as observed in the study of Al Dahoudi [39]. However, the intensity of preferred (002) orientation peak diminished a little because of gallium content due primarily to competing ionic radii of Zn^{2+} (0.074 nm) and Ga^{3+} (0.062 nm), respectively. As all other conditions were similar, it is only the difference in composition and respective ionic radii that rendered films their polycrystalline characters.

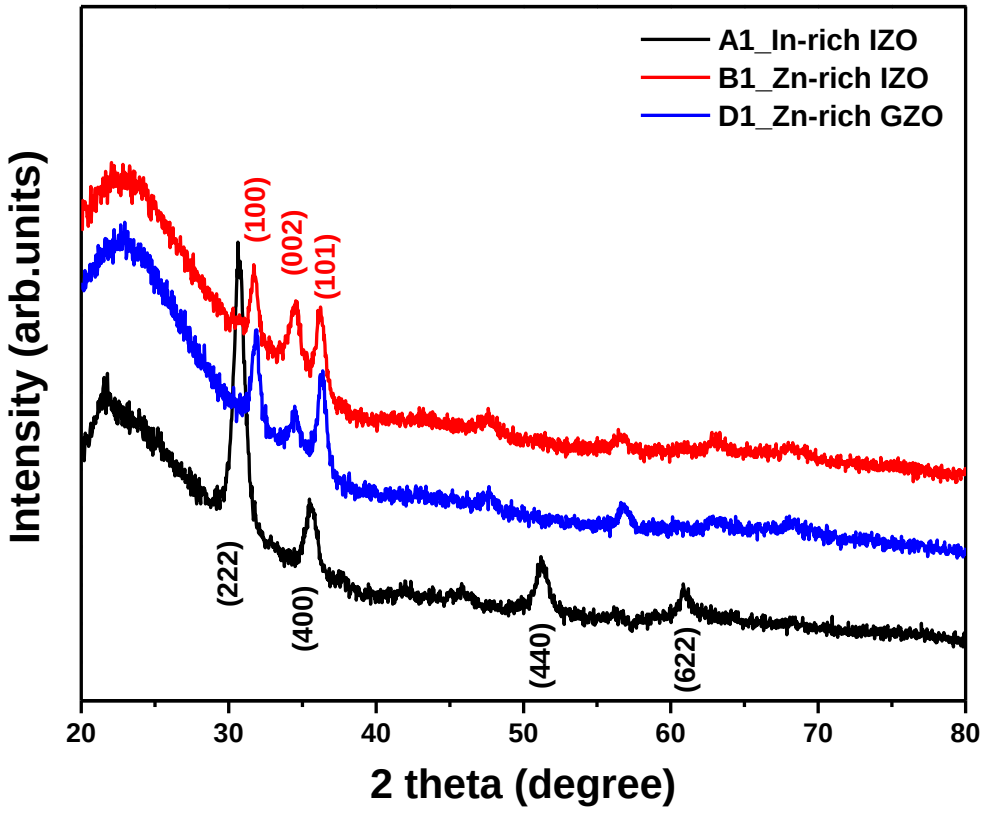

Figure 2. XRD patters obtained for indium-rich IZO (A1), zinc-rich IZO (B1), and zinc-rich GZO (D1) samples in the case of RTA in a vacuum.

3.2. UV/VIS/NIR Optical Measurements

Thin-film precursor solutions were obtained by mixing oxide source solutions in different proportions as given in Table 1 and the process detailed in Section 2.1. All oxide source solutions were of 0.5 M concentration. Furthermore, thin films were prepared following the same deposition procedure as detailed in Section 2.2 and all films contained an equal number of layers. In addition, pre and post-deposition consolidation and annealing treatments were also the same for all deposited films. In addition to thickness, precursor solutions concentration, and composition contribute to the resistivity and transparency of the prepared films. Other than composition, all precursors were of the same concentration, prepared films, therefore, were of a similar thickness of 200 nm. This is, therefore, the only difference in the composition that could affect physical and chemical properties of films. Transparency and conductivity are usually in inverse relation where one increases as the other decreases. Both these facts were shown by the films when characterized for optical behavior.

Figure 3 shows optical transmission behavior of films characterized in the range of 200–900 nm. All films showed an average optical transmission of more than 80% in the visible from 400 to 800 nm. The decrease in transmission from 300 to 200 nm with decreasing wavelengths is attributed to the optical band gap at lower wavelengths [44]. The optical response of all films remained on an average similar. This commonality of optical response is believed to relate with stable crystalline structures appearing for all thin films. Stable structures resulted because of homogeneous mixing of oxide source solutions in precursors for A1 films and appearing of a predominately single phase of In_2O_3. Similarly, for B1 and D1 thin films, the predominately stable singular crystalline structure of ZnO appeared, delivering high optical transparency.

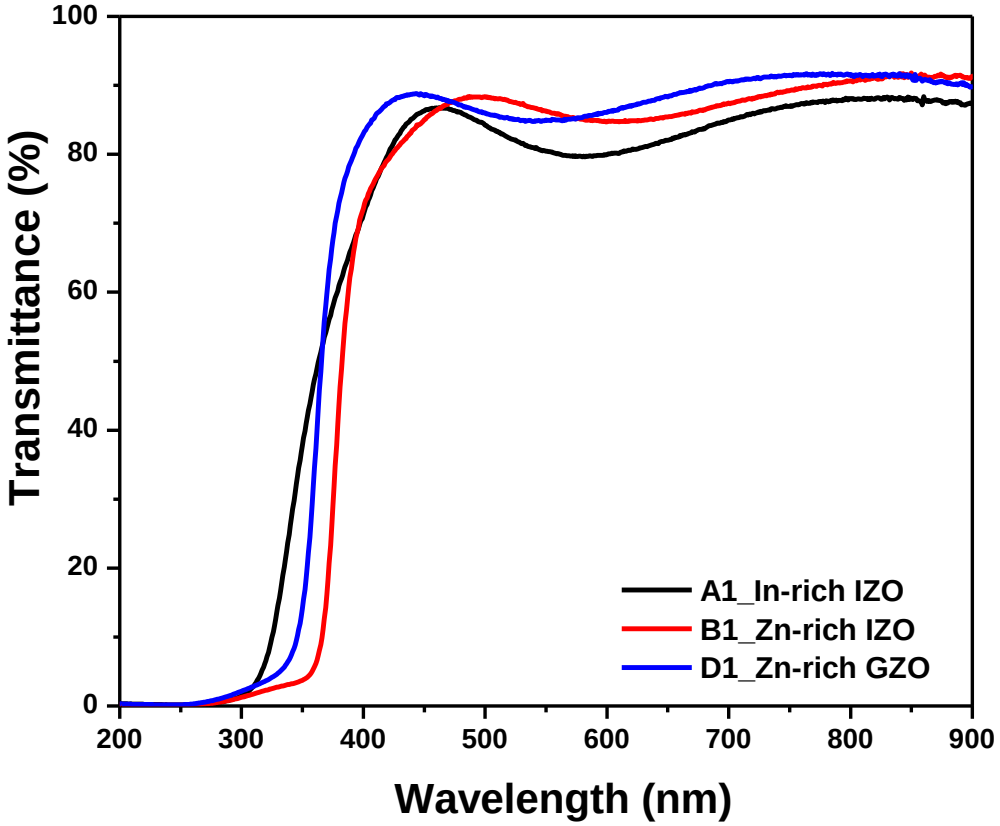

Figure 3. Optical transmission spectra obtained for indium-rich IZO (A1), zinc-rich IZO (B1), and zinc-rich GZO (D1).

3.3. Hall Effect Electrical Measurements

The electrical conductivity of thin films is affected by physical factors like consolidating heating after each layer deposition, post-deposition annealing, and number of layers, hence thickness. There are chemical factors that can influence the electrical behavior of thin films like precursor solution concentration and composition. The precursor solutions were obtained mixing individual oxide source solutions of 0.5 M concentration. Thin films were prepared following similar pre- and post-deposition treatments. Precursor solutions were different only in oxide source solutions mixing ratios. This could be the reason that all films were on average of similar thickness. Films were characterized for electrical resistivity first by using a hand-operated instrument from Jandel Engineering, UK wherein four-probe method is applied. Resistivity values were determined by using formula $\rho = 4.532 \times V/I \times t$. In this formula, 4.532 is correction factor, V is the voltage drop across applied current I and t is film thickness.

Electrical resistivity (sheet and bulk) along with carrier concentration and carrier mobility were measured by self-operating Hall Effect (HE) measuring apparatus using van der Pauw geometry. As per HE measurements, all films showed n-type conductivity. Results for HE measurements are reproduced in Table 2. For A1 thin films, the precursor was obtained mixing oxide source solutions of indium oxide and zinc oxide in a ratio of 1:9. Because of higher indium content and bigger ionic radius, In_2O_3 developed as a pre-dominant single phase in prepared thin films producing minimum structural defects with enhanced crystallinity. Post-deposition annealing in vacuum increased carrier concentration (n) [45] that helped these films to have lower electrical resistivity. Pre-dominant indium oxide single-phase rendered ordered structure in thin films that lowered grain boundary scattering and increased carrier mobility (μ). Resistivity (ρ) is inversely proportional to the product of carrier concentration and carrier mobility, $\rho = 1/ne\mu$ [46].

Table 2. Results for Hall Effect (HE) electrical measurements for indium-rich IZO (A1), zinc-rich IZO (B1), and zinc-rich GZO (D1).

Sample ID	Mixing Ratios	Deposition Technique	Deposition Temperature	Thickness	Resistivity		Hall Mobility	Carrier Concentration	
			(°C)	(nm)	(ohm.sq)	(ohm.cm)	(cm^2/V.s)	sheet (cm^{-2})	bulk (cm^{-3})
A1	IZO (9:1)	Spin coating	400	200	173 167	0.00345 0.00335	11.90 10.80	3.04×10^{15} 3.46×10^{15}	1.53×10^{20} 1.73×10^{20}
B1	IZO (1:9)	Spin coating	400	200	427 400	0.00855 0.00799	12.30 12.20	1.18×10^{15} 1.28×10^{15}	5.91×10^{19} 6.40×10^{19}
D1	GZO (1:9)	Spin coating	400	200	839 624	0.0168 0.0125	6.00 7.28	1.24×10^{15} 1.37×10^{15}	6.29×10^{19} 6.86×10^{19}

Higher product of carrier concentration and carrier mobility helped A1 thin films to have higher electrical conductivity among prepared thin films. In the case of B1 thin films, although oxide source solution mixing ratio was reversed, because of the difference in ionic radii, zinc oxide peaks diminished [42]. This rendered thin films with lower crystallinity, resulting in reduced carrier mobility with lower electrical conductivity. In the case of D1 thin films, wherein almost equal ionic radii of Zn^{2+} and Ga^{3+} competed for crystal growth resulting in further reduced crystallinity and increased scattering reducing carrier mobility and hence electrical conductivity [42]. Highly resistive behavior of C1 thin films (gallium-rich GZO, because of this were not characterized further other than resistivity and not applied in solar cell device) is due to excessive concentration of gallium that leads to a decrease in the degree of crystallinity and conductivity [43], decrease in electron density [47] and suppression of donor oxygen vacancies [48].

For B1 thin films even though the amount of indium oxide source solution was very low in precursor solution (1:9) but because of bigger ionic radius of In^{3+}, ZnO phase could not grow prominently [37], as shown by diminished characteristic peaks in XRD analysis. This resulted in reduced mobility and carrier concentration that resulted in lower electrical conductivity for these films in comparison to A1 thin films. In the case of D1 films with higher ZnO source solution content, singular ZnO crystal structure developed but almost similar ionic radii of Ga^{3+} (0.062 nm) in comparison to Zn^{2+} (0.074 nm) hindered crystal growth and mobility. However, all films developed regularly predominately singular polycrystalline structures, therefore, their optical response remained similar.

3.4. SEM Surface Morphology Analysis

Scanning electron microscopy was performed to observe the surface morphology of thin films. SEM results for A1, B1, and D1 thin films are presented in Figure 4. A1 thin films dominated by single In_2O_3 phase and nano polycrystalline character appeared with a uniform surface. Homogeneous mixing of ZnO into In_2O_3 was facilitated by smaller ionic radii of Zn^{2+} in comparison to In^{3+}. The observation is supported by XRD measurements detailed in Section 3.1. SEM analysis further supports inference made upon XRD measurements in the case of B1 and D1 thin films as well. In the case of B1 thin films, a greater amount of zinc oxide source solution in precursor composition supported the growth of characteristic zinc oxide wurtzite structure. Because of greater ionic radius, In^{3+} did not mix homogeneously in precursor solution and resulted in bit porous morphology with little empty spaces lowering carrier mobility. This scattering behavior of individual oxides is more pronounced in the case of D1 thin films with equal ionic radii of Zn^{2+} and Ga^{3+}. Dominant ZnO characteristic wurtzite structure growth appeared in XRD results (Figure 4), however, scattering increased as shown by reduced carrier mobility.

3.5. Solar Cell Device Measurements

To examine the performance of TCO thin films in the photoelectric conversion process, a complete solar cell with a superstrate structure as depicted in Figure 1 was fabricated. TCO thin films A1, B1, and D1 were applied and J-V characteristics of solar cell were measured. For comparison, a similar

solar cell structure was fabricated with standard FTO TCO thin film (thickness!). Figure 5 shows J-V characteristics for all TCOs prepared in this study along with standard FTO. J-V characterization results for all samples against standard FTO TCO are reproduced in Table 3.

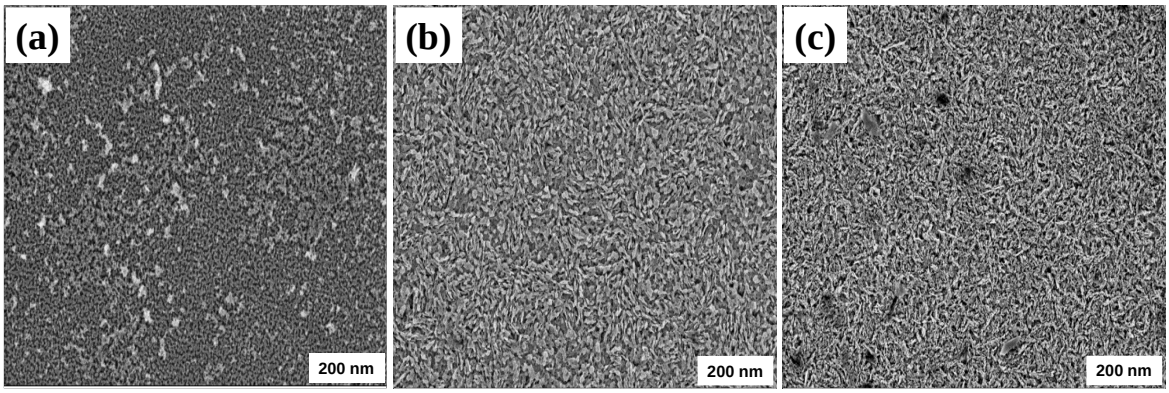

Figure 4. SEM images obtained for thin films, (**a**) indium-rich IZO (A1), (**b**) zinc-rich IZO (B1), and (**c**) zinc-rich GZO (D1).

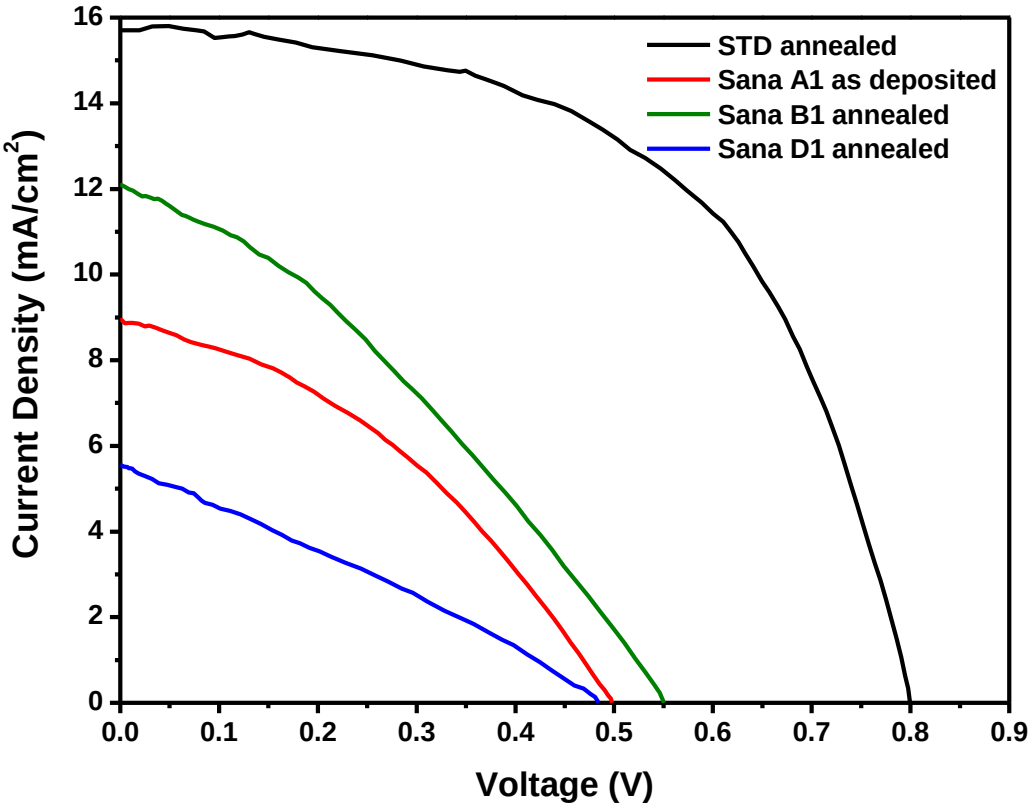

Figure 5. J-V characteristic curves obtained by applying prepared TCOs in comparison to standard FTO.

This is reiterated that all samples were prepared following similar precursor solution and deposition procedures except precursor solution composition. Therefore, it is only the relative composition of oxide source solutions in precursors that rendered TCO thin films their opto-electrical properties. Keeping preparation procedures the same, results suggest that there is plenty of space to enhance J-V characteristics if the relative amount of oxide sources in precursor composition, the number of layers, i.e., the thickness of TCO or pre and post-deposition annealing temperatures or time is increased. As observed, J-V characteristics can further be improved by better filtration of TCO oxide sources and precursor solutions, as shown in Figure 7.

Table 3. J-V photocurrent conversion characteristics for TCOs.

Photo Current Values	Standard TCO	TCO A1	TCO B1	TCO D1
η (%)	6.88	1.66	2.17	0.77
Jsc (mA/cm^2)	15.70	9.00	12.10	5.60
Voc (V)	0.80	0.50	0.55	0.48
FF (%)	54.80	36.8	32.60	28.80
Rsh (Ω.cm)	411.00	142.00	96.00	106.00
Rs (Ω.cm)	12.00	30.00	33.00	67.00

It has been described in Section 3.2 that total transmission characteristics for all samples were better than standard FTO, as also reproduced in Figure 6. Figure 7 shows the surface characteristics of TCOs when employed in the solar cell. TCO characteristics of prepared thin films could be improved by reducing their surface roughness. Leftover residue due to poor filtration of precursor solutions resulted in critical damage to cell junctions. This caused low shunt resistance reducing conversion efficiency of the solar cell. Although overall transmission characteristics of TCOs were better than standard TCO, low thickness and very high sheet resistance resulted in high series resistance of the solar cell.

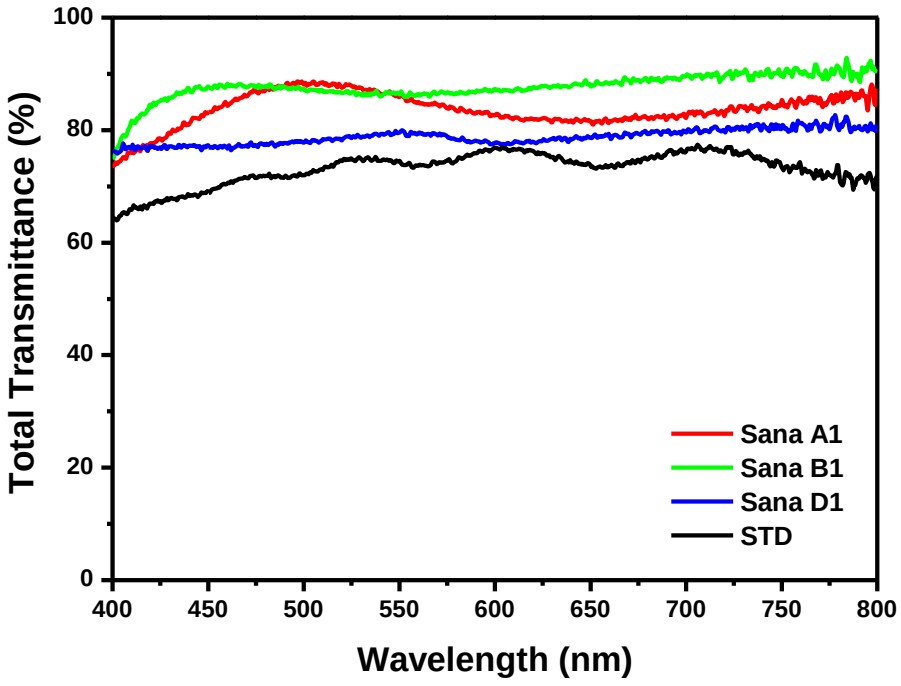

Figure 6. Total transmission observed in comparison to standard TCO for TCO A1, B1, and D1.

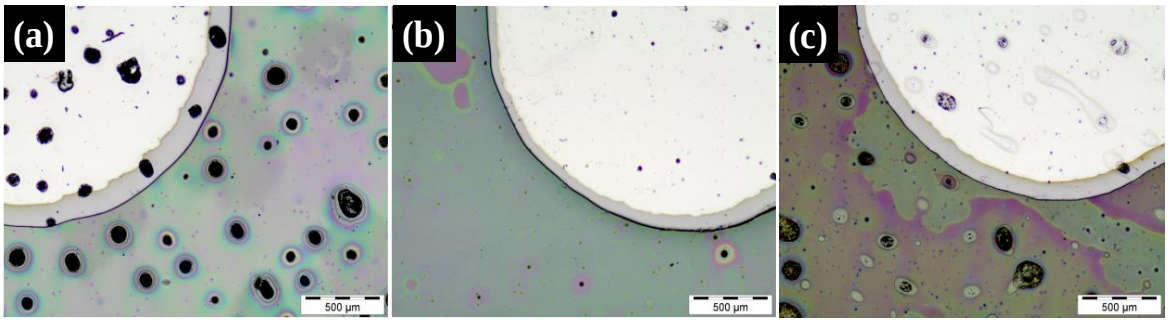

Figure 7. Surface images of the solar cell showing lack of filtration of precursor solutions, (**a**) indium-rich IZO (A1), (**b**) zinc-rich IZO (B1), and (**c**) zinc-rich GZO (D1).

3.6. Substitution or Reduction of Indium Content

Alternative transparent conducting thin films were developed through solution synthesis. An effort was made to prepare thin films with required electrical resistivity and optical transparency of a typical transparent conducting oxide wherein the amount of indium is reduced or substituted altogether. As per the chemical profile given by the US department of health and human services, ITO is available at wt. % ratios (oxide weight ratio or In-Sn atomic ratios) of 90:10 (most common), 95:05 and 80:20 [10]. This work did not do usual "doping" of indium in zinc or vice versa rather used equal molarity concentration oxide source solutions for indium, zinc, and gallium, respectively. Urea as fuel was then mixed in oxide source solutions in molar proportions as detailed in the Experimental Section. These separate oxide source solutions were then mixed in 1:9 and 9:1 proportions to get thin-film precursor solutions. Moreover, wt. % ratio of indium to zinc and gallium to zinc turns out to be 50.2:49.8 and 46.2:53.8, respectively. In terms of atomic and molar ratios, it is 1:1 for indium to zinc and gallium to zinc, respectively. The transparent conducting thin films with required characteristics have been obtained, wherein indium content has successfully been reduced exploiting combustion synthesis and thin films prepared to avoid vacuum deposition.

4. Conclusions

Sustainability is becoming an important consideration for the production of alternative energy. One way to achieve sustainability could be through the development of renewable energy resources and the enhancement of the efficiency of alternative energy technologies. In the field of alternative photovoltaic materials and technologies, sustainability could be pursued through the preparation of alternative materials and reducing the quantity of materials in scarcity like the metal indium. This follows the policy of reducing, reusing, and recycling materials of interest in sustainability. In this research work, we have succeeded in preparing thin films used in solar cells with reduced use of material along with alternatives. Highly transparent and conducting thin films were prepared through spin-coating precursors of metal oxide nitrates exploiting solution combustion chemistry. Combustion synthesis helped the conversion of metal nitrate precursors at low external temperatures. Indium-rich IZO 9:1 precursor resulted in single-phase cubic bixbyite structure of In_2O_3, whereas zinc-rich IZO 1:9 precursor resulted in dominant ZnO hexagonal wurtzite crystal structure. Precursor for zinc-rich gallium GZO 1:9 crystallized in typical ZnO wurtzite hexagonal crystal structure. All films were given similar post-deposition rapid thermal annealing in different controlled environments. Prepared thin films were applied as TCO in a typical silicon-based solar cell and compared for J-V characteristics to FTO. Encouraging results were obtained, keeping in view the comparative thickness of TCOs. Observations suggest that increasing TCO thickness along with better filtration of precursor solutions would help improve surface roughness and sheet resistance of solar cell devices. Strong single-phase crystallization in thin films suggests better TCO characteristics could be achieved combining combustion synthesis and post-deposition rapid thermal annealing. The results obtained are encouraging to achieve enhanced conductivity and transparency through low-cost vacuum-free deposition of alternative TCOs with substituted or reduced use of indium in TCOs for applications in photovoltaic devices.

Author Contributions: Conceptualization, methodology, software, validation, formal analysis, investigation, data curation, writing—original draft preparation, writing—review and editing, S.U.; conceptualization, validation, investigation, resources, writing—original draft preparation, R.B., T.M., and R.M.; conceptualization, methodology, validation, resources, project administration, funding acquisition, supervision, writing—review and editing, E.F.; conceptualization, software, validation, investigation, resources, visualization, supervision, project administration, funding acquisition, writing—original draft preparation, writing—review and editing, T.R. and F.S. All authors have read and agreed to the published version of the manuscript.

Funding: This research received no external funding.

Conflicts of Interest: The authors declare no conflict of interest.

Abbreviations

PV	Photovoltaics
TCO	Transparent conducting oxide
IZO	Indium zinc oxide
GZO	Gallium zinc oxide
SCS	Solution combustion synthesis
RTA	Rapid thermal annealing
GW	Giga Watts
TW	Tera Watts
LCD	Liquid crystal displays
FTO	Fluorine doped tin oxide
Jsc	Short circuit current density
Voc	Cut-off voltage
Rsh	Sheet resistance
XRD	X-rays diffraction
JCPDS	Joint Committee on Powder Diffraction–International Center for Diffraction Data
UV/VIS/NIR	Ultra-violet/visible/near infra-red
HE	Hall Effect
SEM	Scanning electron microscopy
J-V	Current–voltage
FF	Fill factor
Rs	Resistivity
US	United States

References

1. Mozumder, M.S.; Mourad, A.-H.I.; Pervez, H.; Surkatti, R. Recent developments in multifunctional coatings for solar panel applications: A review. *Sol. Energy Mater. Sol. Cells* **2019**, *189*, 75–102. [CrossRef]
2. Photovoltaics Power Systems Program. *IEA PVPS Survey Report: Trends 2018 in Photovoltaic Applications*; International Energy Agency: Paris, French, 2018; pp. 1–86.
3. Photovoltaics Power Systems Program. *IEA PVPS Programme Annual Report 2018*; International Energy Agency: Paris, French, 2018; pp. 1–127.
4. Fortuato, E.; Ginley, D.; Hosono, H.; Paine, D.C. Transparent Conducting Oxides for Photovoltaics. *MRS Bull.* **2007**, *32*, 242–247. [CrossRef]
5. Lu, H.; Ren, X.; Ouyang, D.; Choy, W.C.H. Emerging Novel Metal Electrodes for Photovoltaic Applications. *Small* **2018**, *14*, e1703140. [CrossRef] [PubMed]
6. Ikhmayies, S.J. Transparent Conducting Oxides for Solar Cells. In *Mediterranean Green Buildings and Renewable Energy*; Sayigh, A., Ed.; Springer: Cham, Switzerland, 2017; pp. 899–908.
7. Jayathilake, D.S.Y.; Nirmal Peiris, T.A. Overview on Transparent Conducting Oxides and State of the Art of Low-Cost Doped Zinc Oxide Systems. *SF J. Mater. Chem. Eng.* **2018**, *1*, 1004.
8. Minami, T. New n-Type Transparent Conducting Oxides. *MRS Bull.* **2000**, *25*, 38–44. [CrossRef]
9. Thiele, C.; Das, R. "Transparent Conductive Films (TCF) 2012-2022: Forecasts." Technologies, Players. Available online: https://www.idtechex.com/zh/research-report/transparent-conductive-films-tcf-2012-2022-forecasts-technologies-players/307 (accessed on 1 December 2020).
10. National Toxicology Program. *Chemical Information Profile for Indium Tin Oxide*; National Institute of Environmental Health Sciences, US Department of Health and Human Services: Washington, DC, USA, 2009; pp. 1–31.
11. Alberi, K.; Nardelli, M.B.; Zakutayev, A.; Mitas, L.; Curtarolo, S.; Jain, A.; Fornari, M.; Marzari, N.; Takeuchi, I.; Green, M.L.; et al. The 2019 materials by design roadmap. *J. Phys. D Appl. Phys.* **2018**, *52*, 013001. [CrossRef]
12. Chen, Y.; Meng, F.; Ge, F.; Xu, G.; Huang, F. Ga-doped ZnO films magnetron sputtered at ultralow discharge voltages: Significance of controlling defect generation. *Thin Solid Films* **2018**, *660*, 840–845. [CrossRef]

13. Tondare, R.S.; Shivaraj, B.W.; Narasimhamurthy, H.N.; Krishna, M.; Subramanyam, T.K. Effect of deposition time on structural, electrical and optical properties of aluminium doped zinc oxide thin films by RF magnetron sputtering. *Mater. Today Proc.* **2018**, *5*, 2710–2715. [CrossRef]
14. Ferdaous, M.T.; Shahahmadi, S.A.; Sapeli, M.M.I.; Chelvanathan, P.; Akhtaruzzaman, M.; Tiong, S.K.; Amin, N. Interplay between variable direct current sputtering deposition process parameters and properties of ZnO:Ga thin films. *Thin Solid Films* **2018**, *660*, 538–545. [CrossRef]
15. Tsai, D.-C.; Chang, Z.-C.; Kuo, B.-H.; Wang, Y.; Chen, E.-C.; Shieu, F.-S. Thickness dependence of the structural, electrical, and optical properties of amorphous indium zinc oxide thin films. *J. Alloys Compd.* **2018**, *743*, 603–609. [CrossRef]
16. Maeng, W.J.; Park, J.-S. Growth characteristics and film properties of gallium doped zinc oxide prepared by atomic layer deposition. *J. Electroceram.* **2013**, *31*, 338–344. [CrossRef]
17. Kaushik, V.K.; Mukherjee, C.; Sen, P.K. ZnO based transparent thin film transistor grown by aerosol assisted chemical vapour deposition. *J. Mater. Sci. Mater. Electron.* **2018**, *29*, 15156–15162. [CrossRef]
18. Park, J.; Lee, G.; Kwon, Y.Y.; Park, K.; Lee, J.; Jin, Y.W.; Nah, Y.; Kim, H. Enhancement in light extraction efficiency of organic light emitting diodes using double-layered TCO structure. *Org. Electron.* **2014**, *15*, 2178–2183. [CrossRef]
19. Ivanova, T.; Harizanova, A.; Koutzarora, T.; Vertruyen, B.; Stefanov, B. Structural and morphological characterization of sol-gel ZnO: Ga films: Effect of annealing temperatures. *Thin Solid Films* **2018**, *646*, 132–142. [CrossRef]
20. Bouaine, A.; Bourebia, A.; Guendouz, H.; Riane, Z. Synthesis and characterization of In doped ZnO thin film as efficient transparent conducting oxide candidate. *Optik* **2018**, *166*, 317–322. [CrossRef]
21. Kumar, K.D.A.; Ganesh, V.; Shkir, M.; AlFaify, S.; Valanarasu, S. Effect of different solvents on the key structural, optical and electronic properties of sol–gel dip coated AZO nanostructured thin films for optoelectronic applications. *J. Mater. Sci. Mater. Electron.* **2017**, *29*, 887–897. [CrossRef]
22. Dintle, L.K.; Luhanga, P.V.; Moditswe, C.; Muiva, C.M. Compositional dependence of optical and electrical properties of indium doped zinc oxide (IZO) thin films deposited by chemical spray pyrolysis. *Phys. E Low-Dimens. Syst. Nanostruct.* **2018**, *99*, 91–97. [CrossRef]
23. Devasia, S.; Athma, P.V.; Shaji, M.; Kumar, M.S.; Anila, E.I. Post-deposition thermal treatment of sprayed ZnO:Al thin films for enhancing the conductivity. *Phys. B Condens. Matrer* **2018**, *533*, 83–89. [CrossRef]
24. Edinger, S.; Bansal, N.; Bauch, M.; Wibowo, R.A.; Újvári, G.; Hamid, R.; Trimmel, G.; Dimopoulos, T. Highly transparent and conductive indium-doped zinc oxide films deposited at low substrate temperature by spray pyrolysis from water-based solutions. *J. Mater. Sci.* **2017**, *98*, 41301–48602. [CrossRef]
25. Way, A.; Luke, J.; Evans, A.D.; Li, Z.; Kim, J.; Durrant, J.R.; Lee, H.K.H.; Tsoi, W.C. Florin doped tin oxide as an alternative of indium tin oxide for bottom electrode of semi-transparent organic photovoltaic devices. *AIP Adv.* **2019**, *9*, 085220. [CrossRef]
26. Özgür, Ü.; Hofstetter, D.; Morkoç, H. ZnO Devices and Applications: A Review of Current Status and Future Prospects. *Proc. IEEE* **2010**, *98*, 1255–1268. [CrossRef]
27. Ullah, S.; Branquinho, R.; Santa, A.; De Matteis, F.; Martins, R.; Davoli, I.; Gonçalves, G.; Fortunato, E.; Golçalves, G. Boosting highly transparent and conducting indium zinc oxide thin films through solution combustion synthesis: Influence of rapid thermal annealing. *Semicond. Sci. Technol.* **2018**, *33*, 105004. [CrossRef]
28. Ullah, S.; De Matteis, F.; Davoli, I. Rapid Thermal Annealing for Solution Synthesis of Transparent Conducting Aluminum Zinc Oxide Thin Films. *J. Electron. Mater.* **2017**, *46*, 6609–6616. [CrossRef]
29. Vasile, N.; Iftimie, S.; Acsente, T.; Locovei, C.; Călugăr, A.I.; Radu, A.; Ion, L.; Antohe, V.-A.; Manica, D.; Toma, O.; et al. Physical properties of indium zinc oxide and aluminium zinc oxide thin films deposited by radio-frequency magnetron sputtering. *Mater. Res. Express* **2020**, *6*, 126447. [CrossRef]
30. Arulkumar, S.; Parthiban, S.; Dharmalingam, G.; Salim, B.; Kwon, J.Y. Environmentally Stable, Solution-Processed Indium Boron Zinc Oxide Thin-Film Transistors. *J. Electron. Mater.* **2020**, *49*, 5606–5612. [CrossRef]
31. Shan, F.; Guo, H.-B.; Kim, H.-S.; Lee, J.-Y.; Sun, H.-Z.; Choi, S.G.; Koh, J.-H.; Kim, S.-J. Enhanced Electrical Performance of Structurally Engineered Memristor Devices with Multi-Stacked Indium Zinc Oxide Films. *Phys. Status Solidi (A)* **2020**, *217*, 1900967. [CrossRef]

32. Kang, J.H.; Song, A.; Park, Y.J.; Seo, J.H.; Walker, B.; Chung, K. Tungsten-Doped Zinc Oxide and Indium–Zinc Oxide Films as High-Performance Electron-Transport Layers in N–I–P Perovskite Solar Cells. *Polymers* **2020**, *12*, 737. [CrossRef]
33. Ruzgar, S.; Caglar, Y.; Caglar, M. The influence of low indium composition ratio on sol–gel solution-deposited amorphous zinc oxide thin film transistors. *J. Mater. Sci. Mater. Electron.* **2020**, *31*, 11720–11728. [CrossRef]
34. Branquinho, R.; Santa, A.; Carlos, E.; Salgueiro, D.A.L.; Martins, R.; Fortunato, E. Solution Combustion Synthesis: Applications in Oxide Electronics. *Dev. Combust. Technol.* **2016**, *397*, 397–417.
35. González-Cortés, S.L.; Imbert, F.E. Fundamentals, properties and applications of solid catalysts prepared by solution combustion synthesis (SCS). *Appl. Catal. A Gen.* **2013**, *452*, 117–131. [CrossRef]
36. Branquinho, R.; Salgueiro, D.; Santos, L.; Barquinha, P.; Pereira, L.; Martins, R.; Fortunato, E. Aqueous Combustion Synthesis of Aluminum Oxide Thin Films and Application as Gate Dielectric in GZTO Solution-Based TFTs. *ACS Appl. Mater. Interfaces* **2014**, *6*, 19592–19599. [CrossRef] [PubMed]
37. Jain, S.; Adiga, K.; Verneker, V.P. A new approach to thermochemical calculations of condensed fuel-oxidizer mixtures. *Combust. Flame* **1981**, *40*, 71–79. [CrossRef]
38. Epifani, M.; Melissano, E.; Pace, G.; Schioppa, M. Precursors for the combustion synthesis of metal oxides from the sol–gel processing of metal complexes. *J. Eur. Ceram. Soc.* **2007**, *27*, 115–123. [CrossRef]
39. Al Dahoudi, N. Comparative study of highly dense aluminum- and gallium-doped zinc oxide transparent conducting sol-gel thin films. *Bull. Mater. Sci.* **2014**, *37*, 1243–1248. [CrossRef]
40. Gong, L.; Liu, Y.; Gu, X.; Lu, J.; Zhang, J.; Ye, Z.; Chen, Z.; Li, L. Study on the thermal stability of Ga-doped ZnO thin film: A transparent conductive layer for dye-sensitized TiO2 nanoparticles based solar cells. *Mater. Sci. Semicond. Process.* **2014**, *26*, 276–281. [CrossRef]
41. Chen, T.-H.; Liao, T.-Y. Influence of Annealing Temperature on the Characteristics of Ti-Codoped GZO Thin Solid Film. *J. Nanomater.* **2013**, *2013*, 1–6. [CrossRef]
42. Nayak, P.K.; Yang, J.; Kim, J.; Chung, S.; Jeong, J.; Lee, C.; Hong, Y. Spin-coated Ga-doped ZnO transparent conducting thin films for organic light-emitting diodes. *J. Phys. D Appl. Phys.* **2009**, *42*, 035102. [CrossRef]
43. Vorobyeva, N.A.; Rumyantseva, M.N.; Vasiliev, R.B.; Kozlovskii, V.F.; Soshnikova, Y.M.; Filatova, D.G.; Baranchikov, A.E.; Ivanov, V.K.; Gaskov, A.M. Effect of heterovalent substitution on the electrical and optical properties of ZnO(M) thin films (M=Ga, In). *Russ. J. Inorg. Chem.* **2014**, *59*, 403–412. [CrossRef]
44. Taylor, M.P.; Readey, D.W.; Van Hest, M.F.A.M.; Teplin, C.W.; Alleman, J.L.; Dabney, M.S.; Gedvilas, L.M.; Keyes, B.M.; To, B.; Perkins, J.D.; et al. The Remarkable Thermal Stability of Amorphous In-Zn-O Transparent Conductors. *Adv. Funct. Mater.* **2008**, *18*, 3169–3178. [CrossRef]
45. Lee, H.-W.; Cho, W.-J. Effects of vacuum rapid thermal annealing on the electrical characteristics of amorphous indium gallium zinc oxide thin films. *AIP Adv.* **2018**, *8*, 015007. [CrossRef]
46. Igasaki, Y.; Saito, H. The effects of zinc diffusion on the electrical and optical properties of ZnO:Al films prepared by r.f. reactive sputtering. *Thin Solid Film.* **1991**, *199*, 223–230. [CrossRef]
47. Hu, J.; Gordon, R.G. Atmospheric pressure chemical vapour deposition of gallium doped zinc oxide thin films from diethyl zinc, water and triethyl gallium. *J. Appl. Phys.* **1992**, *72*, 5381–5392. [CrossRef]
48. Hosono, H. Ionic amorphous oxide semiconductors: Material design, carrier transport, and device application. *J. Non-Cryst. Solids* **2006**, *352*, 851–858. [CrossRef]